

To appear in *The Universe As Seen By ISO*, ed. P. Cox and M. F. Kessler

HEATING THE GAS IN PHOTODISSOCIATION FRONTS

B. T. Draine¹ and Frank Bertoldi^{2,3}

¹Princeton University Observatory, Princeton, NJ 08544, USA

²Max-Planck-Institut für Radioastronomie, Bonn, Germany

³Max-Planck-Institut für Extraterrestrische Physik, Garching, Germany

ABSTRACT

ISO has provided us with a new perspective on gas temperatures in photodissociation regions through measurements of line emission from rotationally-excited levels of H₂. The H₂ rotational level populations provide a thermal probe, showing that gas temperatures $T_{gas} \approx 500 - 1000$ K prevail in a portion of the PDR where significant H₂ is present. Such high gas temperatures were unexpected. Theoretical models for the S140 PDR are presented. Possible mechanisms for heating the gas to such high temperatures are discussed.

Key words: ISO; infrared astronomy; molecular hydrogen.

1. INTRODUCTION

Photodissociation fronts play an important part in the global energetics of star-forming galaxies, as an appreciable fraction of the energy radiated by newly-formed stars is reprocessed in photodissociation fronts, resulting in H₂ and fine structure line emission. If we want to understand the emission spectra of star-forming galaxies, good theoretical models of photodissociation fronts are required.

ISO observations of line emission from rotationally-excited levels of H₂ have provided unequivocal evidence for gas temperatures in the 500 – 1000 K range in a portion of the photodissociation region (PDR) where the H₂ fraction is appreciable. These temperatures were higher than expected from current models of the heating and cooling processes in PDRs, and therefore require reconsideration of the physics of the gas and dust in PDRs.

In §2. we review the basic structure of photodissociation fronts, and in §3. we discuss how H₂ can be used as a thermometer to indicate the gas temperatures in PDRs. In §4. we use the S140 PDR as an example. Theoretical models for the heating and cooling in PDRs are discussed in §5., and in §6. we stress some of the uncertainties in the modelling of PDRs. We summarize in §7.

2. WHAT IS A PHOTODISSOCIATION FRONT?

The term “photodissociation front” refers to the interface separating a region which is predominantly molecular, and a region where the ultraviolet energy density is sufficiently high so that the molecular fraction is $\ll 1$. Young O and B stars located near their natal (only partially-disrupted) molecular clouds produce conspicuous (i.e., high surface brightness) photodissociation fronts. A number of reviews of PDRs have appeared recently (Hollenbach & Tielens 1997, Sternberg *et al.* 1998, Walmsley 1998), including a comprehensive article by Hollenbach & Tielens (1998).

A photodissociation front is not a mathematical surface, but rather an extended “photodissociation region” (PDR). Figure 1 is a cartoon illustrating the different zones within the PDR.

The structure of the PDR is determined primarily by the attenuation of the far-ultraviolet (6 – 13.6 eV) radiation field, as one moves from the ionization front into the PDR. The H₂ abundance results from a balance between formation of H₂ on dust grains and photodissociation of H₂ by $912 < \lambda < 1110\text{\AA}$ photons. The photodissociation rate is determined by both H₂ self-shielding (Draine & Bertoldi 1996) as well as attenuation by dust. Because of this self-shielding, the H/H₂ transition occurs closer to the ionization front than the C⁺/C/CO or O/O₂ transitions. Atoms with ionization potentials lower than H (e.g., C) are photoionized in the PDR, whereas species with ionization potentials greater than H (e.g. O) are neutral in the PDR.

Ionization fronts and dissociation fronts are, in general, time-dependent structures (Bertoldi & Draine 1996). Under many circumstances, however, the structure can be approximated as being stationary in a frame moving with the dissociation front. Furthermore, if the dissociation front is advancing into the molecular gas with a propagation speed $v_{DF} \lesssim 0.3 \text{ km s}^{-1}$ (Bertoldi & Draine 1996), advection terms can be neglected in the equations governing the thermal and chemical conditions: the temperature is effectively determined by a local balance between heating and cooling, and abundances by a local balance between formation and destruction. For

most PDRs this inequality is expected to be satisfied (Bertoldi & Draine 1996, Störzer & Hollenbach 1998), although time dependence may be important for some planetary nebulae (Hollenbach & Natta 1995).

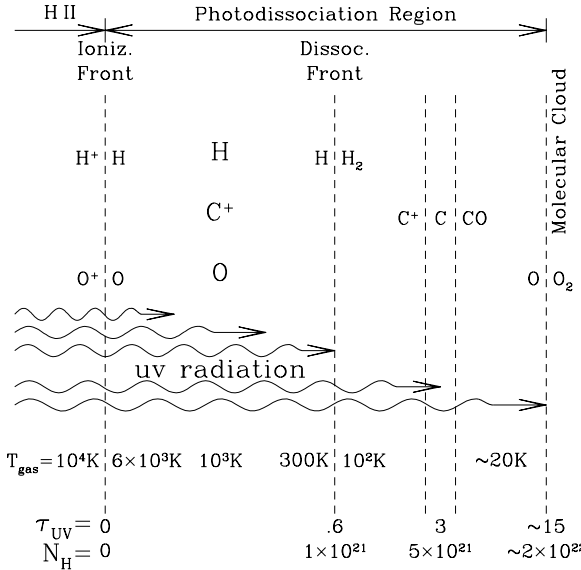
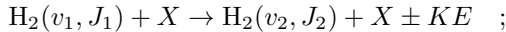


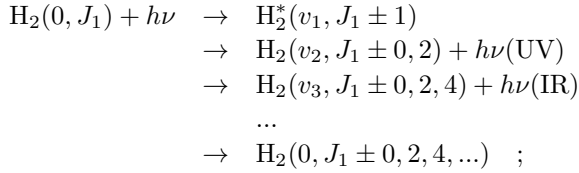
Figure 1. The structure of a PDR produced by radiation from a star which also emits enough ionizing photons to produce an HII region. The ionization front separates the HII region from the PDR. Typical values of the effective far-ultraviolet optical depth, and H nucleon column density are shown.

3. H₂ AS A THERMAL PROBE

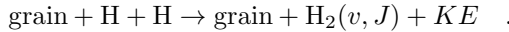
The (v, J) rovibrational excited states of H₂ are populated by inelastic collisions



by UV pumping:



and by formation on grains:



At the densities $n_H \gtrsim 10^4 \text{ cm}^{-3}$ of bright PDRs, collisions maintain the ($v=0, J$) levels of H₂ in approximate thermal equilibrium for $J \lesssim 5$. Therefore measurements with *ISO* of the quadrupole emission line intensities from levels $J \lesssim 5$ provide a good indicator of the gas temperature, while the emission from the higher J levels is sensitive to both the gas temperature and density. We do not expect the level populations to be characterized by a single “excitation

temperature”, but the “best-fit” excitation temperature characterizing a range of J values (e.g., $J=3-5$) should indicate the approximate gas temperature in the part of the PDR where these levels are predominantly excited.

The populations of very high J levels (e.g., $J = 15$) are potentially affected by UV pumping (the quadrupole decay cascade following a UV pump injects a small amount of H₂ into high J states) and formation on dust grains (some fraction of the newly-formed H₂ may be in high J states). Therefore excitation temperatures characterizing $J \gtrsim 10$ may not reflect gas temperatures.

4. THE S140 PDR

ISO obtained spectra of the photodissociation region where the S140 HII region abuts the L1202/L1204 molecular cloud (Timmermann *et al.* 1996); see Figure 2.

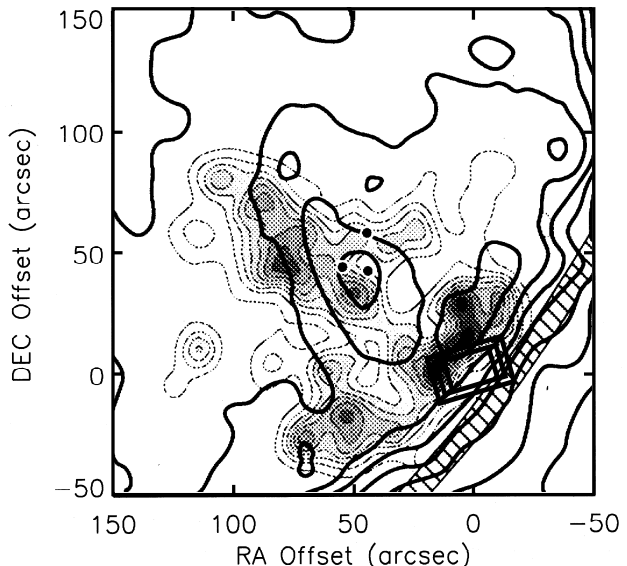


Figure 2. The S140 PDR, where radiation from the B0.5V star HD 211880 impinges on a dense clump in the L1202/L1204 molecular cloud. The ionization front is shown as a shaded region. The greyscale shows [CI]610 μm emission (White & Padman 1991). Contours show CO(3-2) emission (Hayashi *et al.* 1987). The SWS apertures are shown as rectangles positioned just interior to the ionization front, where the photodissociation front is expected to be located, viewed approximately edge-on. The exciting star is located ~ 7 arcmin SW of the aperture. Figure taken from Timmermann *et al.* (1996).

Timmermann *et al.* (1996) reported measurements of line emission out of (0, J) levels with J as large as 9 (see Figure 3). The inferred column densities for $3 \leq J \leq 7$ are characterized by an excitation temperature $T_{\text{exc}} \approx 500 \text{ K}$; the emission from $J = 8$ and 9 suggest a higher temperature. How much of the PDR is characterized by such high temperatures? To address this question, Timmermann *et al.* (1996)

considered an *ad-hoc* temperature profile, shown in Figure 4.

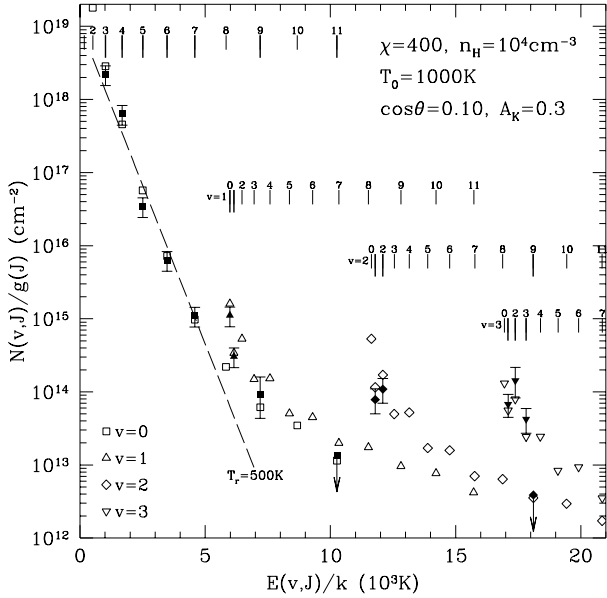


Figure 3. Observed (filled symbols) and model (open symbols) column densities in rovibrational levels of H_2 along the line-of-sight. Observed intensities have been corrected for foreground extinction by dust with 0.3 mag of extinction at K . The PDR is assumed to be inclined with $\cos\theta = 0.1$. The broken line is a $T = 500\text{ K}$ thermal distribution, indicating that a significant amount of H_2 is located in regions where $T_{\text{gas}} \gtrsim 500\text{ K}$. Taken from Timmermann *et al.* (1996).

With this *ad-hoc* temperature profile, the chemical abundances are computed by requiring steady-state balance between formation and destruction, using standard assumptions for the formation rate of H_2 on grains, and a detailed treatment of H_2 self-shielding. H_2 level populations were computed for a plane-parallel PDR, including both UV pumping and collisional excitation and deexcitation (Draine & Bertoldi 1996). The H nucleon density was assumed to be $n_{\text{H}} = 10^4\text{ cm}^{-3}$ (as expected for pressure balance with the HII region), and the radiation field at 1000\AA was assumed to be $\chi = 400$ times stronger than the Habing (1968) value (as expected for the $\sim 1.7\text{ pc}$ distance from the exciting B0.5V star).

The resulting model is shown in Figure 3, where it is assumed that $\cos\theta = 0.1$, where θ is the angle between the line-of-sight and the normal to the model PDR. It is seen that the level populations are in fairly good agreement with observations, although the model overestimates the $v = 1$ and 2 level populations, while underestimating the $v = 3$ levels. For this model, $T = 500\text{ K}$ at the point where $y \equiv 2n(\text{H}_2)/n_{\text{H}} = 0.2$, and $T = 150\text{ K}$ where $y = 0.5$.

Timmermann *et al.* (1996) also compared predicted and observed fine structure line intensities with those predicted by the model. Agreement is generally good, allowing for uncertainties in abundances of Si and Fe: $[\text{CI}]609\text{ }\mu\text{m}$ is close to the observed value, while

$[\text{SiII}]35\text{ }\mu\text{m}$ and $[\text{FeII}]26\text{ }\mu\text{m}$ agree with observations if $\text{Si/H} = 1.5 \times 10^{-6}$ and $\text{Fe/H} = 5 \times 10^{-8}$. The principal discrepancy is $[\text{OI}]63\text{ }\mu\text{m}$, which the model predicts to be ~ 5 times stronger than observed.

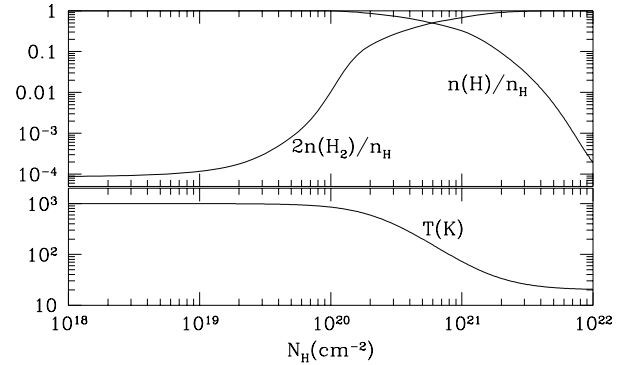


Figure 4. *Ad-hoc* temperature profile adopted for S140 PDR model. With this assumed temperature profile, the H_2 abundances are computed by requiring a balance between H_2 formation and photodissociation. Taken from Timmermann *et al.* (1996).

5. THERMAL BALANCE IN PDRS

The obvious question now is: what temperatures do we *expect* the gas to have in PDRs, if we assume that the gas temperature is determined by a balance between heating and cooling? The principal heating processes in PDRs are:

- Photoelectrons emitted from dust grains;
- UV pumping, followed by collisional deexcitation of rovibrationally excited H_2 ;
- Photodissociation (kinetic energy of $\text{H}+\text{H}$);
- H_2 formation (kinetic energy, collisional deexcitation);
- Photoionization of H, C, etc.

while the dominant cooling processes are:

- fine-structure line emission from $[\text{CII}]158\text{ }\mu\text{m}$, $[\text{OI}]63, 146\text{ }\mu\text{m}$, $[\text{SiII}]35\text{ }\mu\text{m}$, $[\text{FeII}]25\text{ }\mu\text{m}$, ...;
- H_2 quadrupole emission;
- CO rotational emission.

The grain photoelectric heating rate is quite uncertain. Here we show results assuming the photoelectric heating rate of Bakes & Tielens (1994).

The cross sections for collisional excitation and deexcitation of H_2 are also uncertain; for $T_{\text{gas}} > 1000\text{ K}$ we use the $\text{H}-\text{H}_2$ inelastic rates of Martin & Mandy (1995) and Mandy & Martin (1995), while for $T_{\text{gas}} < 1000\text{ K}$ we extrapolate the Mandy & Martin rates using eq. (16) of Draine & Bertoldi (1996), but using

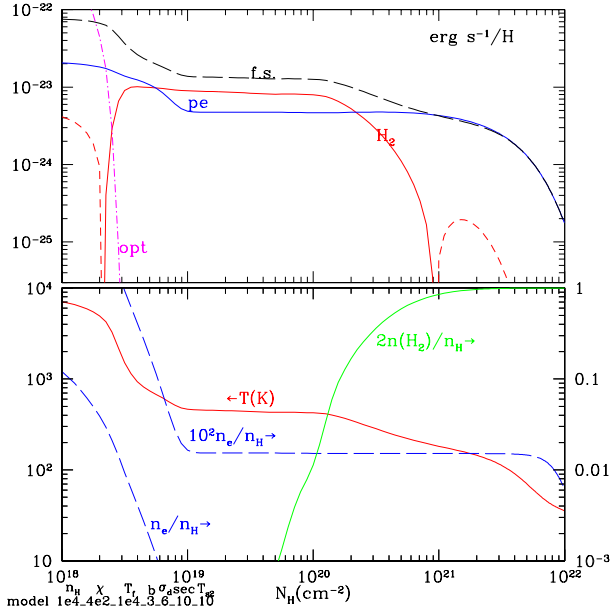


Figure 5. Thermochemical profile of S140 PDR model, with temperatures determined by thermal balance calculations. Lowell panel: gas temperature T , H_2 fraction $2n(H_2)/n_H$, and fractional ionization $n(e)/n_H$. Upper panel: heating (solid lines) and cooling (broken lines) due to grain photoelectric heating (“pe”), the H_2 molecule (including formation, collisional excitation and deexcitation, and photodissociation), fine structure line emission (“f.s.”), and optical line emission (“opt”). Note that H_2 has a net heating effect in much of the PDR.

$\theta = 1000$ K rather than 600 K as the transition temperature, as discussed by Draine & Bertoldi (1999).

The fine-structure line emission is computed using standard collision rates, abundances characteristic of the gas toward ζ Oph (e.g., Si and Fe depleted by factors of 40 and 250, respectively). Some of the lines – in particular, [OI]63 μ m – can become optically thick. An “escape probability” approximation was used to estimate local cooling rates (Draine & Bertoldi 1999).

Figure 5 shows the calculated thermochemical profile, as well as showing the contributions of different processes to heating and cooling. Close to the ionization front the fractional ionization is a few percent, and $T_{\text{gas}} \approx 4000 - 6000$ K; in this region, optical line emission (e.g., [SII]6716,6739) dominates the cooling, but is unimportant when $T_{\text{gas}} \lesssim 4000$ K. Emission from excited fine-structure levels dominates the cooling for $50 \lesssim T_{\text{gas}} \lesssim 4000$ K.

H_2 contributes net heating throughout much of the PDR. This heating arises mainly from collisional deexcitation of rovibrationally excited H_2 following UV-pumping or H_2 formation on grains, with a secondary contribution from the kinetic energy of newly-formed H_2 and $H+H$ following photodissociation. The other major heating process is photoelectric emission from dust grains. Both H_2 heating and photoelectric heating are important for $N_H \lesssim 10^{21} \text{ cm}^{-2}$; beyond this point H_2 self-shielding has reduced the photodissociation rate (and therefore the H_2 formation rate as well) to very low levels, and photoelectric heating dominates.

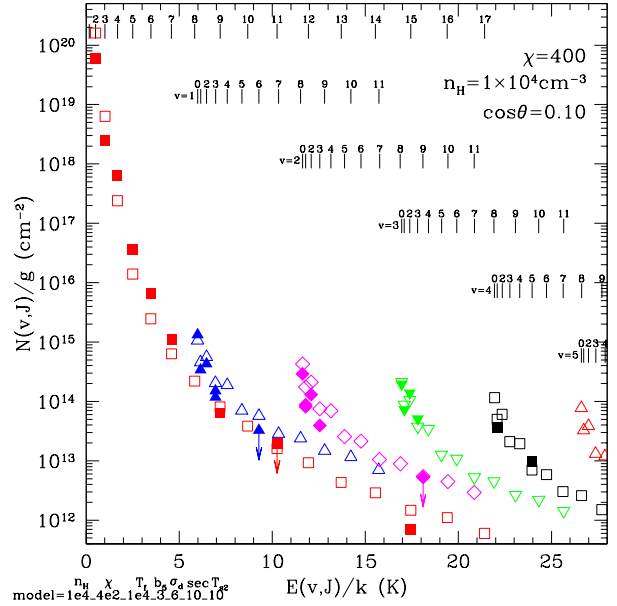


Figure 6. Column densities $N(v, J)$ along the line-of-sight, divided by level degeneracies $g(J)$. Solid symbols: observed values based on line intensities corrected for foreground extinction with $A_K = 0.2$ mag, and internal extinction within the PDR, inclined with $\cos \theta = 0.1$. Open symbols: model for S140 PDR with $\chi = 400$ and $n_H = 10^4 \text{ cm}^{-3}$, with temperatures determined by thermal balance.

Figure 6 shows the observed column densities of excited states of H_2 along the line of sight toward the S140 PDR, corrected for an assumed extinction $A_K = 0.3$ mag. A number of H_2 line detections and upper limits were obtained subsequent to preparation of the Timmermann *et al.* (1996) paper on the S140 PDR; Figure 6 shows column densities obtained from the most recent data reduction (Bertoldi *et al.* 1998). Also shown are the column densities predicted by our model, which assumes an inclination of the PDR with $\cos \theta = 0.1$ – a factor of 10 “limb-brightening”.

There are significant differences between the model H_2 level populations and those observed toward S140. The assumed factor of 10 limb-brightening leads to a good match for the vibrationally excited levels. However, the $v = 0$ column densities predicted by the model fall off too steeply – while the $J = 2, 3$ column densities in the model exceed the observed values by a factor ~ 2 , the $J = 3 - 7$ column densities are too low by factors $\sim 2 - 3$. This presumably indicates that either the H_2 inelastic cross sections or the thermal profile are incorrect. Note, however, that the model appears to be able to reproduce the observed population of H_2 in $J = 15$, and thereby a high excitation temperature for the high- J levels.

Somewhat better agreement can be obtained if the gas density and illuminating radiation field are both increased; in Figures 7 and 8 we show the result of increasing the illuminating radiation field to $\chi = 600$,

and raising the gas density to $n_{\text{H}} = 4 \times 10^4 \text{ cm}^{-3}$. With the increased χ and n_{H} , a good fit to the observed H_2 line intensities is obtained for a limb-brightening factor $1/\cos\theta = 5$. However, the assumed value of χ is somewhat larger than expected from our knowledge of the exciting star, and n_{H} is larger than expected given our estimates of the pressure in the ionization front (Timmermann *et al.* 1996). It should also be noted that even with these values of χ and n_{H} , there are still noticeable discrepancies between model and observation. It is difficult to match the low observed line ratio between 0-0S(1) and 0-0S(2). Both lines are in the same size *ISO* aperture, so beam dilution differences could not be the cause of the mismatch. The model also overproduces $J = 15$, although this line was observed after *ISO*'s helium boiloff, which made its flux calibration more difficult. Most other levels' column densities are well reproduced.

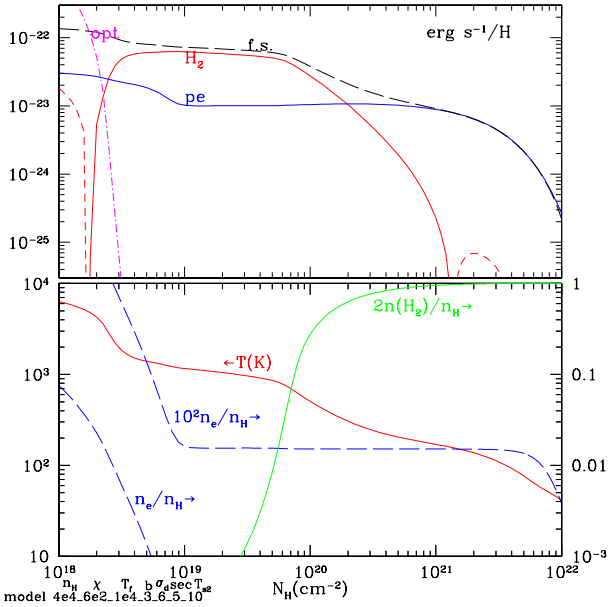


Figure 7. Same as Fig. 5, but for $n_{\text{H}} = 4 \times 10^4 \text{ cm}^{-3}$ and $\chi = 600$.

The high gas temperatures found in S140 are not unique. Early evidence for high gas temperatures in PDRs was obtained from H_2 $J = 3-1$ and $4-2$ line observations by Parmar *et al.* (1991), who inferred $T_{\text{gas}} = 1000 \pm 250 \text{ K}$ at a position .0244 pc from the ionization front in the Orion Bar, and $T_{\text{gas}} = 600 \pm 50 \text{ K}$ another .0044 pc farther away from the ionization front.

High gas temperatures near the H/H_2 transition were inferred, based on ground-based spectra, for the reflection nebula NGC 2023 (Draine & Bertoldi 1996). *ISO* spectra of the reflection nebula NGC 7023 (Bertoldi *et al.* 1999) and the Orion Bar (Rosenthal *et al.* 1999), also show that some of the H_2 must be in a region of gas temperatures $T_{\text{gas}} \gtrsim 600 \text{ K}$.

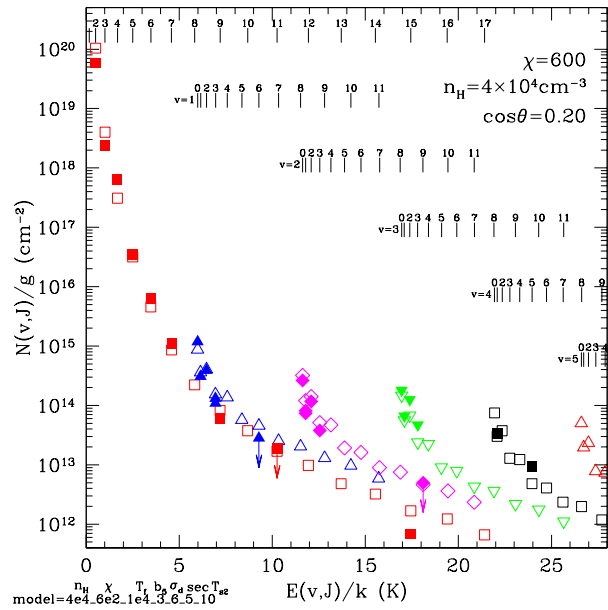


Figure 8. Same as Fig. 6, but for $n_{\text{H}} = 4 \times 10^4 \text{ cm}^{-3}$ and $\chi = 600$, and with the PDR assumed to be inclined with $\cos\theta = 0.2$.

6. WHAT NEEDS TO BE CHANGED IN THE MODELS?

Where do we stand on modeling the H_2 emission from PDRs? Considering that the emission arises from a region with a range of densities, one might take the point of view that we are doing pretty well – our constant density planar PDR models can approximately reproduce the observed level populations using ultraviolet pumping of H_2 plus collisional excitation/deexcitation, with gas temperatures obtained from a balance of heating and cooling. Nevertheless, it seems to us that the discrepancies between our best models and the observations are unacceptably large. The discrepancies may be due in part to our underlying assumptions of planar geometry and uniform density, but may also be due to poor approximations in our description of the local microphysics of heating, cooling, chemistry, and level excitation. Below we indicate some of the areas where existing models may require modification.

6.1. H_2 inelastic collision cross sections

The $\text{H}-\text{H}_2$ collisional excitation/deexcitation rates used here for $T_{\text{gas}} \gtrsim 600 \text{ K}$ are those of Martin & Mandy (1995) and Mandy & Martin (1995), which were obtained from quasi-classical trajectory calculations. These rates are thought to be accurate for $T_{\text{gas}} \gtrsim 600 \text{ K}$, but are likely to be increasingly inaccurate at low temperatures, where quantum calculations are required (Flower 1997, Forrey *et al.* 1997). Forrey *et al.* (1997) have recently reported accurate rates for $\Delta J = \pm 2$ transitions among the $v = 0$, $J = 0-5$ levels, for $100 < T_{\text{gas}} < 1000 \text{ K}$; our extrapolation from the Mandy & Martin (1995) results was

adjusted to give good agreement with these newer rates.

While H-H₂ inelastic rates are generally larger than for H₂-H₂ collisions, the latter are important when the H fraction becomes small. Quantum calculations have recently been reported by Flower (1997).

6.2. Grain Photoelectric Heating Rate

The thermal models reported here employ a photoelectric heating rate recommended by Bakes & Tielens (1994) for heating by 6-13.6 eV photons:

$$\Gamma_{pe} = n_H \sigma_{uv} u_{uv} c \epsilon$$

$$\begin{aligned} \sigma_{uv} &= \text{dust EUV absorption/H} \approx 6 \times 10^{-22} \text{ cm}^2 \\ u_{uv} &= \text{EUV energy density} = \chi \times 0.033 \text{ eV cm}^{-3} \\ \epsilon &= \text{photoelectric heating efficiency} \\ &= .049(1. + x/1925)^{-0.73} + \\ &\quad .037 T_4^{0.7}(1. + x/5000)^{-1} \\ x &\equiv \chi(T/K)^{0.5}/(n_e/\text{cm}^{-3}) \end{aligned}$$

Bakes & Tielens assumed a “MRN” power-law size distribution down to ultrasmall grains containing only ~ 30 carbon atoms (i.e., PAH molecules). Since we have only an imprecise understanding of the composition and size distribution of the grains, this heating rate is necessarily uncertain. Under the conditions of interest (e.g., the point where $2n(H_2)/n_H = 0.1$ in Figure 5), we have $\chi \approx 400$, $n_e \approx 1.5 \text{ cm}^{-3}$, and $T \approx 350 \text{ K}$, so that $x \approx 5000$, and the heating efficiency $\epsilon \approx 0.021$, which increases further into the cloud to $\epsilon \approx 0.049$. Since photoelectric emission from grains is a dominant heating process in PDRs, its further study would be of value.

6.3. Dust-to-Gas Ratio

The dust grains play a crucial role in photodissociation regions. In particular, they determine the rate for formation of H₂ from H, and, as seen above, photoelectric emission from dust is a major heat source. Common practice is to adopt a “standard” dust-to-gas ratio and wavelength-dependent dust opacity in the PDR. However, Weingartner & Draine (1999) have pointed out that the anisotropic radiation in a PDR can drive the grains through the gas at drift velocities which may be comparable to the flow velocity of the gas relative to the dissociation front, thereby leading to an *increase* in the dust-to-gas ratio in the PDR, at least for those grain compositions and sizes for which the grain-gas drift velocities are large. Increased dust concentrations in part of the PDR could alter the thermochemical properties of the PDR by increasing the H₂ formation rate (and therefore the local rate of UV pumping and photodissociation of H₂) and by increasing the grain photoelectric heating rate. As a result, we can expect that the gas temperature will be increased near the photodissociation front.

The anisotropic radiation incident on a dust grain results in a force which consists of the “ordinary” radiation pressure force due to absorption and scattering, plus additional forces due to anisotropic photoelectron emission (the “illuminated” side of the grain will emit more photoelectrons per second than the “dark” side) and anisotropic photodesorption (adsorbed H or H₂ can be photodesorbed, with a larger rate on the “illuminated” side of the grain). The recoil force from photoelectric emission and photodesorption can be several times larger than the “ordinary” radiation pressure (Weingartner & Draine 1999).

Because the grains are charged, drift across the magnetic field lines will be inhibited. It will be of great interest to see the extent to which these effects will change the dust-to-gas ratio, and the grain size distribution, in the PDR, and how this affects the thermochemical profile of the PDR.

7. SUMMARY

ISO has opened a new window on photodissociation fronts, by allowing us to measure the populations of the rotationally-excited levels of the $v = 0$ state of H₂, thereby placing strong constraints on the gas temperature. The S140 PDR provides an excellent illustration of this capability.

The observed line emission from rotationally-excited levels of H₂ indicates that gas temperatures $T_{\text{gas}} \gtrsim 500 \text{ K}$ prevail in part of the PDR where appreciable H₂ is present. Attempts to construct theoretical models of the PDR tend to fall short in terms of the populations of levels $J = 3 - 7$,

We discuss the uncertainties in the dominant heating and cooling mechanisms; the H₂ inelastic collision rates still have significant uncertainties, and the grain photoelectric heating rate is yet not well-established. In addition, it appears possible that the dust-to-gas ratio in PDRs such as S140 may deviate from the “standard” value since the anisotropic radiation field can drive the grains through the gas with significant drift speeds.

ACKNOWLEDGEMENTS

For their contribution to the recent S140 data analysis we are grateful to the MPE SWS group, and especially to H. Feuchtgruber and E. Wiprecht. This research was supported in part by NSF grant AST 96-19429 (BTD) and by the Deutsche Forschungsgemeinschaft (FB). B.T.D. wishes to thank Osservatorio Arcetri for its gracious hospitality during the completion of part of this work.

REFERENCES

Bakes, E.L.O., Tielens, A.G.G.M. 1994, ApJ, 427, 822

Bertoldi, F., *et al.* 1998, private communication

Bertoldi, F., Draine, B.T. 1996, ApJ, 458, 222

Bertoldi, F., Feuchtgruber, H., *et al.* 1999, in preparation

Draine, B.T., Bertoldi, F. 1996, ApJ, 468, 269

Draine, B.T., Bertoldi, F. 1999, in preparation

Flower, D.R. 1997, MNRAS, 288, 627

Forrey, R.C., Balakrishnan, N., Dalgarno, A., & Lepp, S. 1997, ApJ, 489, 1000

Habing, H.J. 1968, Bull. Astron. Inst. Netherlands, 19, 421

Hayashi, M., Hasegawa, D., Omodaka, D., *et al.* 1987, ApJ, 312, 327

Hollenbach, D.J., Natta, A. 1995, ApJ, 455, 133

Hollenbach, D.J., Tielens, A.G.G.M. 1997, ARA&A, 35, 179

Hollenbach, D.J., Tielens, A.G.G.M. 1998, Rev. Mod. Phys., in press

Mandy, M.E., Martin, P.G. 1995, ApJS, 86, 199

Martin, P.G., Mandy, M. 1995, ApJ, 455, L89

Parmar, P.S., Lacy, J.H., Achtermann, J.M. 1991, ApJ, 372, L25

Rosenthal, D., *et al.* 1999, private communication

Sternberg, A., Yan, M., Dalgarno, A. 1998, in *Molecules in Astrophysics: Probes and Processes*, ed. E. van Dishoeck, p. 141

Störzer, H., Hollenbach, D.J. 1998, ApJ, 495, 853

Timmermann, R., Bertoldi, F., Wright, C.M., *et al.* 1996, A&A, 315, L281

Walmsley, C.M. 1998, Astr. Lett. & Comm., 37, 1

White, G.J., Padman, R. 1991, Nature, 354, 511

Weingartner, J.C., Draine, B.T. 1999, this volume